Materials Research. 2018; 21(suppl. 2): e20170869
DOI: http://dx.doi.org/10.1590/1980-5373-MR-2017-0869

Mechanical Loss Angle Measurement for Stressed thin Film Using Cantilever Ring-Down Method

Ling-Chi Kuo[a], Huang-Wei Pan[a], Shu-Yu Huang[a], Shiuh Chao[a]*

[a]*Institute of Photonics Technologies, National Tsing Hua University, 30013, Hsinchu, Taiwan*

Received: September 27, 2017; Revised: February 23, 2018; Accepted: April 20, 2018

Mechanical loss of the coating materials, and hence thermal noise from the mirror coatings, is a limiting factor for the sensitivity of the laser interferometer gravitational waves detector at its most sensitive frequency range. Mechanical loss of the thin films are often measured using the cantilever ring-down method. But when the thin film is under stress, the regular ring-down method gives incorrect results. We report a method to obtain the mechanical loss of stressed thin film using the cantilever ring-down technique. A proof-of-concept example is given to demonstrate and verify our method. The method can also be applied to obtain the mechanical loss angle of a rough interface; an example showed that loss angle of the interface between silicon nitride film deposited by plasma enhanced chemical vapor deposition method and silicon substrate is highly frequency dependent.

Keywords: *mechanical loss angle, laser interferometer gravitational waves detector, mirror coatings, stressed thin film.*

1. Introduction

Sensitivity of the current laser interference gravitational waves detector at its most sensitive frequency region ~100 Hz is limited by the thermal noise of the mirror coatings[1]. Thermal noise is related to the mechanical loss angle through the fluctuation-dissipation theorem[2]. Therefore, studying the mechanical loss of the coating materials is crucial for the development of better coatings of the detector. Cantilever ring-down is a common method for measuring the mechanical loss of coatings[3]. A cantilever, usually silicon, with a thicker clamping pad is fabricated and the coating is deposited on one side of the thinner cantilever. The cantilever is clamped on the pad and excited under vacuum at its resonant frequencies. The decay time of the free damping is recorded and the loss angle is obtained through Eq.1. The loss angle of the film can be deduced from the difference between coated and un-coated cantilevers[4]. The dimensions of the cantilever are designed such that the resonant frequencies fall in the range of interest, i.e. from several tens to several thousand Hz. The thickness of the cantilever is usually about 100 μm or less[5]. The pad needs to be thick enough to avoid energy coupling between the clamp and the cantilever during the ring-down measurement[6]. To fabricate the cantilever one starts with a double-side polished thick silicon wafer, using a lithographic method and KOH etching on one-side to form the cantilever of the desired thickness[7]. The resulting cantilever substrate, shown in Fig. 1(a), is polished on one side and roughened by the KOH etching on the other, the roughness was typically 7.7 nm as was measured by atomic force microscopy (AFM). The coating is then deposited on the polished side of the cantilever for the ring-down measurement.

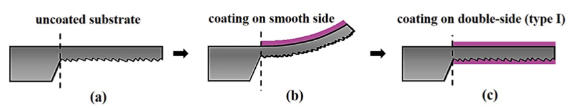

Figure 1. Curvature variation of the samples with double-side coatings on one-side roughened and the other side polished cantilever.

When the coating is stressed, the coated cantilever warps as shown in Fig. 1(b), which may lead to inaccurate ring-down measurement. To eliminate the warping, we propose coating the cantilever on both sides to balance the stress as shown in Fig. 1(c). However, the film on each side is different in the sense that one film is deposited on the smooth surface and the other film is deposited on the roughened surface. We developed a method to separate the loss angle of the film on the smooth surface from that of the double-side coatings. Our method can also be applied to evaluate the additional loss angle of the rough interface between the film and the substrate. Examples are given to demonstrate the validity of our methods.

2. Sample Configuration

Two types of cantilever samples were prepared. Type I is a double-side coated cantilever which is one-side roughened while the other side is left polished as shown in Fig. 1(a) and (c). Type II is a double-side coated cantilever which is roughened on both sides of the substrate as shown in Fig. 2(a) and (c). The roughness on both sides have to be created under exactly the same condition such that they are identical in roughness. After the stressed film is deposited on one side at an elevated temperature, due to differential

*e-mail: schao@ee.nthu.edu.tw

thermal expansion, the cantilever warps on cooling down as shown in Fig. 1(b) and Fig. 2(b). When coating the film on the second side, the cantilever is brought up to the same elevated temperature and the differential thermal expansion stress is released so that the cantilever becomes flattened. On cooling down after the second coating, the cantilever remains flat due to stress balance. The resultant sample configurations are shown in Fig. 1(c) and 2(c) and referred to as type I and type II.

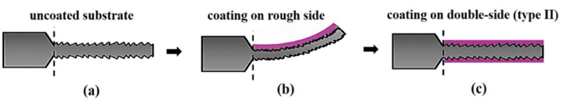

Figure 2. Curvature variation of the samples with double-side coatings on both-side roughened cantilever.

3. Loss Angle Calculation

The loss angle φ is defined as the ratio of the oscillation energy dissipation per cycle to the elastic stored energy[8]:

$$Q^{-1} = \varphi = \frac{1}{\omega}\frac{P}{E} = \frac{2}{\omega\tau} \qquad (1)$$

where P is the power dissipation, E is the stored energy, ω is the angular frequency and τ is the decay time for the resonant mode at ω.

The loss angles of the one-side roughened bare cantilever, φ_s, double-side roughened bare cantilever $\varphi_{s'}$, type I cantilever φ_I, and type II cantilever φ_{II} are shown in Table 1. Because the roughness of the interface is much less than the thickness of the film and the thickness of the substrate is much larger than that of the film, we can approximate $E_s \approx E_{s'}$, $E_f \approx E_{f'}$, and $E_s \gg E_f$. Under these assumptions, the loss angles can be approximated as shown in Table 1.

The total power dissipation in the sample is the sum of the power dissipation of all components. It is simple to show from Table 1, the loss angle of the film that is coated on the polished side, φ_f, is

$$\varphi_f = \frac{1}{\omega}\frac{P_f}{E_f} \approx \frac{E_s}{E_f}\left[(\varphi_I - \varphi_s) - \frac{1}{2}(\varphi_{II} - \varphi_{s'})\right] \qquad (2)$$

Notice that the loss angles in the parentheses can be obtained by direct ring-down measurement on the four samples in Table 1.

When the cantilever is excited with the bending modes, the energy ratio can be approximated as[9,10]:

$$\frac{E_s}{E_f} = \frac{Y_s t_s}{3Y_f t_f} \qquad (3)$$

where Y_s, Y_f are the Young's moduli, and t_s, t_f are the thicknesses of the substrate and the film, respectively. When the cantilever is excited at the torsional mode, the Young's moduli Y_s, Y_f should be replaced by shear moduli G_s, G_f[11].

One would need to prepare one-side roughened bare cantilever s, double-side roughened bare cantilever s', double-side coated cantilever type I and double-side coated cantilever type II samples and measure the loss angles, φ_s, $\varphi_{s'}$, φ_I, φ_{II}, to extract φ_f. The Young's modulus and shear modulus of the silicon substrate, Y_s and G_s, can be obtained from the literature[12]. The Young's modulus of the films, Y_f, can be measured by using instruments such as nano-indenter. If the films are amorphous, i.e. homogeneous and isotropic, shear modulus of the films, G_f, can be obtained from the Young's modulus through the following equation[13], assuming that the Poisson ratio of the films, υ_f, is known:

$$G_f = \frac{Y_f}{2(1+\upsilon_f)} \qquad (4)$$

The loss angle of the rough interface can also be obtained as follows. The film f' which is deposited on the rough surface can be decomposed, in terms of power dissipation and energy stored, into two parts as shown in Fig. 3. One part of the film which is smooth on both surfaces and the other part is the rough interface. Following the method of derivation of Eq. 2, the loss angle of the interface, φ_r, can be obtained as:

$$\varphi_r = \frac{1}{\omega}\frac{P_r}{E_r} \approx \frac{E_f}{E_r}(\varphi_{f'} - \varphi_f) \qquad (5)$$

where

$$\varphi_{f'} = \frac{1}{\omega}\frac{P_{f'}}{E_{f'}} \approx \frac{1}{2}\frac{E_s}{E_f}(\varphi_{II} - \varphi_{s'}) \qquad (6)$$

$\varphi_{f'}$ is the loss angle of the one-side-rough film. When the cantilever is excited with a bending mode, the energy ratio is approximated as:

$$\frac{E_f}{E_r} = \frac{Y_f t_f}{3Y_r t_r} \qquad (7)$$

When the cantilever is excited at the torsional mode, the Young's moduli Y_f, Y_r should be replaced by shear moduli G_f, G_r.

E_r is the energy stored in the rough interface, Y_r is the effective Young's modulus of the interface, we assume Y_r can be taken as the average of the Young's modulus of the film and the substrate. The same assumption holds for the shear modulus of the rough interface G_r. t_r is the effective thickness of the interface that can be taken as the roughness of the surface.

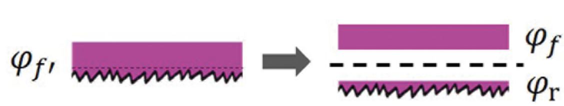

Figure 3. The one-side-rough film f' can be decomposed, in terms of power dissipation and energy stored, into the smooth film f and the rough interface r.

Table 1. Mechanical loss of different samples.

	mechanical loss
 s	$\varphi_s = \frac{1}{\omega}\frac{P_s}{E_s}$
 s'	$\varphi_{s'} = \frac{1}{\omega}\frac{P_{s'}}{E_{s'}} \approx \frac{1}{\omega}\frac{P_{s'}}{E_s}$
type I  f s f'	$\varphi_I = \frac{1}{\omega}\frac{P_s + P_f + P_{f'}}{E_s + E_f + E_{f'}} \approx \frac{1}{\omega}\frac{P_s + P_f + P_{f'}}{E_s}$
type II 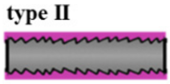 f' s' f'	$\varphi_{II} = \frac{1}{\omega}\frac{P_{s'} + P_{f'} + P_{f'}}{E_{s'} + E_{f'} + E_{f'}} \approx \frac{1}{\omega}\frac{P_{s'} + P_{f'} + P_{f'}}{E_s}$

s One-side roughened bare cantilever
s′ Double-side roughened bare cantilever
f Film on smooth surface
f′ Film on rough surface

4. Proof of Concept

4.1 Loss angle of the stressed silicon nitride film

The photo-lithographic method was used followed by KOH etching to fabricate one-side and two-side roughened cantilevers. The surface roughness of the commercial double-side polished silicon wafer is usually < 0.5 nm, and the KOH etching produced surface roughness of 7.7 nm. Plasma enhanced chemical vapor deposition (PECVD) was used to deposit the silicon nitride film on the cantilevers[14]. The film was amorphous as was revealed by its electron diffraction pattern. The thickness of the film was 199 ± 1 nm. The composition of the film was $SiN_{0.65}$, measured by X-ray photoelectron spectroscopy (XPS). The Young's modulus was 131.6 ± 4.8 GPa, measured by nano-indenter. The Poisson ratio was taken as 0.25[15]. The Young's modulus and shear modulus of the silicon substrate were taken as 169 GPa and 79.6 GPa[12], respectively. The one-side coated cantilever warped with the coating on the concave face indicating tensile stress of the film. The stress was 256.7 ± 6.6 MPa, measured by a curvature meter and calculated by using the Stoney equation[16]. The value and the rms error were obtained from five measurements along five diameters on a coated 4" silicon wafer. The double-side coated cantilever was flat, with the radius of curvatures > 10^3 m before and after double-side coating, indicating that good balance of the stresses was achieved. The loss angles, φ_s, $\varphi_{s'}$, φ_I, and φ_{II}, were measured and the loss angle of the film φ_f was calculated according to the method described. Fig. 4 shows the loss angle of the film, in the black square, for five modes of the cantilever.

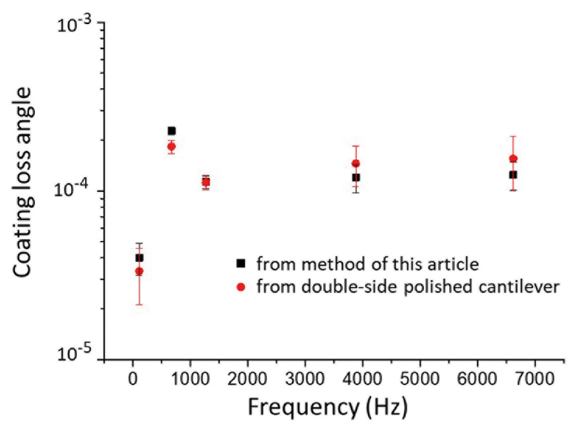

Figure 4. The loss angle of $SiN_{0.65}$ deduced by different methods.

In order to verify our method, we developed a technique to fabricate a double-side polished cantilever with clamping pad from a silicon-on-insulator (SOI) wafer[17]. The double-side polished cantilever had the same dimensions as the regular silicon cantilevers and the surface roughness was < 0.5 nm for both sides. We then deposited the same films on both sides of the cantilever and measured the loss angle of the film using the ring-down method. The result is shown in Fig. 4 as the red dots. The loss angles of the film on regular silicon cantilevers deduced using our method are nearly the same, within the error bars, of the measurement as that form the double-side polished cantilever. However, The SOI wafer is much more expensive than the regular silicon wafer and it is more complicated to fabricate into the shape of the cantilever that routine usage for our purpose is discouraged.

4.2 Loss angle of the rough interface

The film for this example was the same as the previous example except that the composition was $SiN_{0.87}$. The thickness of the film was 219 ± 1 nm. The Young's modulus was 138.0 ± 4.7 GPa. The tensile stress was 423.4 ± 5.9 MPa. Type I and II samples were fabricated and all the relevant loss angle were measured and calculated. The loss angle of the rough interface, φ_r, can then be calculated according to Eq.6. The result is shown in Fig. 5. The roughness of the interface created by KOH etching for this sample was 7.7 nm as was measured by using an atomic force microscope (AFM). Fig. 5 hints that the mechanical loss of the rough interface is highly frequency dependent. However, the full interpretation of Fig. 5 is outwith the scope of this paper.

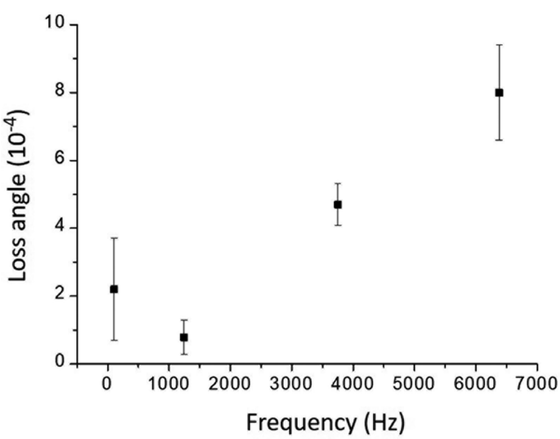

Figure 5. The loss angle of the rough interface at different frequencies.

5. Conclusion

We proposed a method to obtain the mechanical loss angle of a stressed thin film which is coated on a cantilever with surface roughness. We showed that the method is effective by demonstration through an example. Our method can also be applied to obtain the effective mechanical loss angle of a rough interface between a film and a substrate. The measurements show that the mechanical loss angle of the rough interface appears to be highly frequency dependent.

6. Acknowledgement

The works of this paper were supported by the Ministry of Science and Technology of Taiwan, the Republic of China, under the contract 103-2221-E-007-064-MY3. The authors wish to thank the comments from the Optics Working Group of the LIGO Scientific Collaboration.

7. References

1. Abbott BP, Abbott R, Abbott TD, Abernathy MR, Acernese F, Ackley K, et al.; LIGO Scientific Collaboration and Virgo Collaboration. GW150914: The Advanced LIGO Detectors in the Era of First Discoveries. *Physical Review Letters*. 2016;116(13):131103.
2. Callen HB, Welton TA. Irreversibility and Generalized Noise. *Physical Review*. 1951;83(1):34-40.
3. Reid S, Cagnoli G, Crooks DRM, Hough J, Murray P, Rowan S, et al. Mechanical Dissipation in Silicon Flexures. *Physics Letters A*. 2006;351(4-5):205-211.
4. Berry BS, Pritchet WC. Vibrating Reed Internal Friction Apparatus for Films and Foils. *IBM Journal of Research and Development*. 1975;19(4):334-343.
5. Elmer FJ, Dreier M. Eigenfrequencies of a rectangular atomic force microscope cantilever in a medium. *Journal of Applied Physics*. 1997;81(12):7709-7714.
6. Quinn TJ, Speake CC, Davis RS, Tew W. Stress-dependent damping in Cu-Be torsion and flexure suspensions at stresses up to 1.1 GPa. *Physics Letters A*. 1995;197(3):197-208.
7. Chao S, Ou JS, Huang V, Wang J, Wang S, Pan H, et al. Progress of coating development at NTHU. In: *LSC-Virgo Collaboration Meeting*; 2012 Sep 10-14; Rome, Italy. LIGO Technical Document LIGO-G1200849.
8. Nowick AS, Berry BS. Characterization of Anelastic Behavior. In: Nowick AS. *Anelastic Relaxation in Crystalline Solids*. New York: Academic Press; 1972. p. 1-29.
9. Nishino Y, Asano S. The constitutive equations for internal friction in thin-layer materials. *Physica Status Solid (A)*. 1993;139(2):K97-K100.
10. Crooks DRM. *Mechanical loss and its significance in the test mass mirrors of gravitational wave detectors*. [PhD Thesis]. Glasgow: University of Glasgow; 2002.
11. White BE Jr., Pohl RO. Internal friction of subnanometer a-SiO_2 films. *Physical Review Letters*. 1995;75(24):4437-4439.
12. Hopcroft MA, Nix WD, Kenny TW. What Is the Young's Modulus of Silicon? *Journal of Microelectromechanical Systems*. 2010;19(2):229-238.
13. Landau LD, Lifshitz EM, eds. *Theory of Elasticity*. 3rd ed. Oxford: Pergamon Press; 1986.
14. Pan HW, Kuo LC, Wu MY, Huang SY, Juang YH, Chao S. Room Temperature Mechanical Loss of Silicon Nitride-Silica Quarter-Wave Stacks Deposited by Plasma Enhanced Chemical Vapor Deposition (PECVD) Method. In: *LSC-Virgo Collaboration Meeting*; 2016 Aug 29-Sep 1; Glasgow, UK. LIGO Technical Document LIGO-G1601702.
15. Walmsley BA, Liu Y, Hu XZ, Bush MB, Dell JM, Faraone L. Poisson's Ratio of Low-Temperature PECVD Silicon Nitride Thin Films. *Journal of Microelectromechanical Systems*. 2007;16(3):622-627.
16. Stoney GG. The tension of metallic films deposited by electrolysis. *Proceedings of the Royal Society A*. 1909;82(563):172-175.
17. Pan HW, Chen HC, Kuo LC, Chao S. Double-side polished silicon cantilever fabricated from silicon-on-insulator (SOI) wafer. In: *LSC-Virgo Collaboration Meeting*; 2017 Mar 13-16; Pasadena, CA, USA. LIGO Technical Document LIGO-G1700302.